Effect of Solvent on the $O_2(a^1\Delta_g) \rightarrow O_2(b^1\Sigma_g^+)$ Absorption Spectrum: Demonstrating the Importance of Equilibrium vs Nonequilibrium Solvation

Niels Dam,[†] Tamás Keszthelyi,[†,§] Lars K. Andersen,[†] Kurt V. Mikkelsen,[‡] and Peter R. Ogilby*[,†]

Department of Chemistry, University of Aarhus, Langelandsgade 140, DK-8000 Århus, Denmark, and Department of Chemistry, University of Copenhagen, Universitetsparken 5 DK-2100, Copenhagen, Denmark

Received: January 14, 2002

In a time-resolved infrared spectroscopic study, the $a^1\Delta_g \rightarrow b^1\Sigma_g^+$ absorption spectrum of molecular oxygen at ~5200 cm^{-1} was recorded in 19 solvents using a step-scan Fourier transform infrared spectrometer. Solvent-dependent changes in the full width at half-maximum of this absorption band covered a range of ~30 cm^{-1} and solvent-dependent changes in the position of the band maximum covered a range of ~55 cm^{-1}. When considered along with solvent-dependent $O_2(a^1\Delta_g) \rightarrow O_2(X^3\Sigma_g^-)$ emission data, the current results identify features that must be incorporated in computational models of the interaction between oxygen and the surrounding solvent. In particular, data presented herein clearly demonstrate the importance of considering the influence of equilibrium and nonequilibrium solvation when interpreting the effect of solvent on transitions between the $X^3\Sigma_g^-$, $a^1\Delta_g$, and $b^1\Sigma_g^+$ states of oxygen. The data indicate that the bandwidths of the $O_2(a^1\Delta_g) \rightarrow O_2(b^1\Sigma_g^+)$ and $O_2(a^1\Delta_g) \rightarrow O_2(X^3\Sigma_g^-)$ transitions principally reflect the effects of equilibrium solvation, whereas the associated solvent-dependent spectral shifts reflect the effects of both equilibrium and nonequilibrium solvation. These general conclusions make it possible to resolve some long-standing problems associated with early attempts to interpret the effect of solvent on electronic transitions in oxygen

Introduction

In recent years, it has become increasingly apparent that the effect of solvent on radiative transitions in dissolved oxygen provides an informative system to investigate mechanisms by which a host medium can perturb a solute.[1−3] Oxygen is particularly important in this regard because transitions between the three lowest electronic states, the $X^3\Sigma_g^-$, $a^1\Delta_g$, and $b^1\Sigma_g^+$ states, are formally forbidden as electric dipole processes. Thus, for dissolved oxygen, the solvent plays an integral role in defining both the transition probability as well as the transition energy. This point has become quite evident, as increasingly sophisticated spectroscopic experiments have been able to quantify, with greater accuracy, the response of a given transition in oxygen to solvent perturbation. Furthermore, oxygen and many common solvent molecules are sufficiently small that high-level computational tools can be employed to model experimental results. This latter point is a critical component of ultimately establishing accurate mechanisms by which solvent influences the behavior of what is arguably one of nature's most ubiquitous solutes; molecular oxygen.

There are three electronic transitions in dissolved oxygen for which solvent-dependent spectra can be "readily" obtained (Scheme 1). An extensive amount of data on the a → X phosphorescent transition at ~7850 cm^{-1} has been compiled over the years by a number of research groups.[4−7] The effect of solvent on the b → a fluorescence spectrum at ~5200 cm^{-1} has likewise been studied.[8] In these latter experiments, however, the range of solvents from which data can be obtained is limited due to the comparatively short lifetime of the $b^1\Sigma_g^+$ state in solvents that contain C−H and O−H bonds (τ < 100 ns).[9] Finally, we have recently established that the a → b absorption spectrum at ~5200 cm^{-1} can be recorded in time-resolved experiments.[2,10,11] In this case, the comparatively long solvent-

SCHEME 1

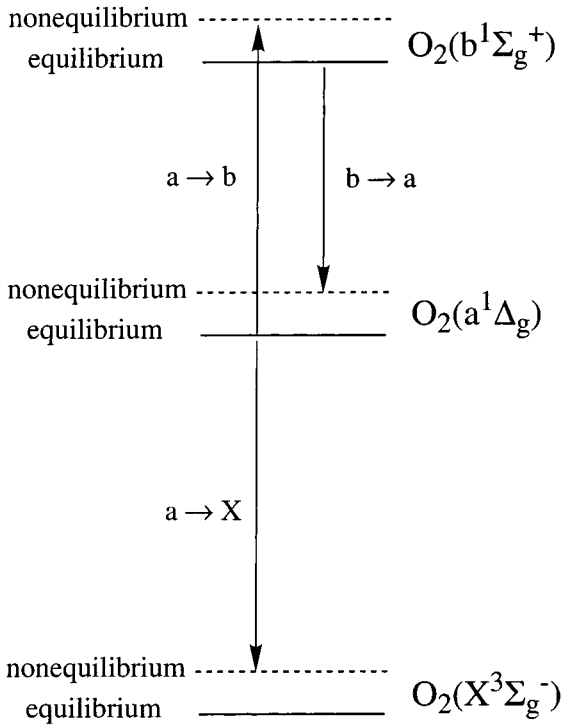

* To whom correspondence should be addressed.
† Department of Chemistry, University of Aarhus.
§ Present address: Surface Spectroscopy Group, Chemical Research Centre, P.O. Box 17, H-1525 Budapest, Hungary.
‡ Department of Chemistry, University of Copenhagen.

10.1021/jp0200876 CCC: $22.00
Published on Web 05/02/2002

dependent lifetime of the $a^1\Delta_g$ state ($\tau > 4\ \mu s$) is an asset in detecting absorbance changes that can be quite small [$\Delta A \sim (0.05-1.0) \times 10^{-3}$].

In considering the role of the solvent on any spectroscopic transition, including these in oxygen, it is important to recognize that the total solvent polarization vector **P** is the sum of two vectors: the optical polarization $\mathbf{P}_{op}$ and the inertial polarization $\mathbf{P}_{in}$ vectors.[12-14] The optical polarization vector $\mathbf{P}_{op}$ represents the response from the solvent electronic degrees of freedom and, because of its short relaxation time, is assumed to always be in equilibrium with the charge distribution of the solute. Functions of the optical dielectric constant ϵ_{op} can be used to represent $\mathbf{P}_{op}$. [ϵ_{op} is the square of the solvent refractive index *n*, determined at optical frequencies (e.g., the sodium D line).] The inertial polarization vector $\mathbf{P}_{in}$ represents the response from the solvent nuclear degrees of freedom (i.e., vibrational, rotational, and translational motion) and remains fixed during an electronic transition. General functions used to represent $\mathbf{P}_{in}$ depend on the difference between the solvent's static dielectric constant ϵ_{st} and ϵ_{op}, although other parameters may be included to account for specific solvent effects.[15,16]

The three transitions shown in Scheme 1 originate from states that are in equilibrium with the surrounding solvent. Specifically, for all solvents of experimental concern, the lifetimes of both the $a^1\Delta_g$ and $b^1\Sigma_g^+$ states are sufficiently long compared to solvent inertial relaxation times. Thus, upon the formation of $O_2(a^1\Delta_g)$ and $O_2(b^1\Sigma_g^+)$ in a pulsed-laser photosensitized reaction in which the sensitizer's excitation energy is transferred to $O_2(X^3\Sigma_g^-)$, $\mathbf{P}_{in}$ is able to respond to the charge distribution of the $a^1\Delta_g$ and $b^1\Sigma_g^+$ states well before that state is probed in a spectroscopic experiment. In contrast, each transition shown in Scheme 1 results in the production of a Franck−Condon state that is not in equilibrium with the surrounding solvent. Although $\mathbf{P}_{op}$ will rapidly respond to the change in the solute charge distribution engendered by the electronic transition, this condition of nonequilibrium solvation will remain until inertial polarization vectors, $\mathbf{P}_{in}$, can likewise react to the change in solute charge distribution.

Despite several early attempts,[6,7,17,18] an all-encompassing model has yet to be presented that satisfactorily accounts for the effect of solvent on the spectral shifts and bandwidths of transitions between the $X^3\Sigma_g^-$, $a^1\Delta_g$, and $b^1\Sigma_g^+$ states in oxygen. However, in a series of recent reports, we established the framework of a correlated ab initio model that appears to be quite promising.[11,19,20] The key components of this model include (1) a molecular complex between one solvent molecule M and O_2 that accounts for short-range solvent−solute interactions, (2) immersion of this M−O_2 complex in a dielectric continuum to account for long-range Coulombic interactions, and (3) consideration of both equilibrium and nonequilibrium solvation. With this approach, ab initio computations were successfully used to model solvent effects on a → X spectral shifts as well as on a−b Stokes shifts.[11,20]

On the basis of our initial studies, we identified several items that would need further attention in the quest to better understand fundamental features of the oxygen-solvent interaction. On the theoretical front, we felt it was necessary to more accurately represent specific solvent effects (e.g., the effects of "inhomogeneities" in the solvation shell) on the spectroscopic and optical properties of a solute. We consequently developed a combined quantum mechanics/molecular mechanics approach that can be used to model a variety of both linear and nonlinear solute properties.[21-23] On the experimental front, it was evident that critical solvent-dependent information on the a → b transition in oxygen was lacking. Specifically, it was necessary to ascertain the effect of solvent on a → b spectral shifts and absorption bandwidths. In the present study, we set out to address this latter issue.

Experimental Section

Details of the method used to record time-resolved a → b absorption spectra at ∼5200 cm^{-1} are given elsewhere.[2,11] Briefly, the $a^1\Delta_g$ state of oxygen was created upon pulsed-laser irradiation of a photosensitizer with energies that were typically ∼ 1−3 mJ $pulse^{-1}$. The laser (Quanta-Ray GCR 230 Nd:YAG) was operated at a 10 Hz repetition rate, and the irradiation wavelength was tuned using (1) the second and third harmonics of the Nd:YAG fundamental output, (2) an optical parametric oscillator (Quanta-Ray MOPO 710) whose output could also be frequency-doubled, or (3) a high-pressure cell of H_2 gas as a Raman shifting medium. Singlet oxygen absorption spectra were recorded using a modified Bruker model IFS-66v/s step-scan FT spectrometer equipped with a 77 K InSb detector. Modification details are likewise provided elsewhere.[2,11,24] The wavenumber scale automatically established by the FTIR with an internal laser was verified using known spectral transitions in water vapor at ∼5200 cm^{-1}.[25] Solvent-dependent $O_2(a^1\Delta_g)$ lifetimes obtained from these time-resolved absorption experiments were all consistent with data obtained from a → X emission experiments.[26]

To obtain both accurate and precise values of the a → b absorption band maximum (∼±1 cm^{-1}) and bandwidth (∼±2 cm^{-1}), it was necessary to record spectra with a reasonably large signal-to-noise ratio. To this end, a given spectrum was typically obtained using the sum of ∼300 time slices of the time-resolved a → b signal, the latter having been obtained using 16−32 coadditions of the data recorded at each FTIR mirror position. The ∼300 time slices used to construct the spectrum represent a ∼7−8 μs segment of the time-resolved singlet oxygen signal that, in turn, was chosen from a domain where the signal level was large (i.e., immediately following the irradiating laser pulse). No less than 10 spectra thus recorded were then added together to yield the final spectrum used for data analysis. All data were recorded using the FTIR spectrometer "resolution" setting of 8 cm^{-1}. However, identical peak maxima and bandwidths were obtained when "resolution" settings of 4 as well as 16 cm^{-1} were used. A change in the bandwidth could only be detected when a "resolution" setting of 32 cm^{-1} was used. The time-dependent changes in sample absorbance typically monitored were on the order of $1-2 \times 10^{-3}$ absorbance units. In methanol and acetonitrile, however, absorbance changes on the order of $\sim(3-5) \times 10^{-4}$ were recorded. These latter changes are due, in part, to smaller a → b molar absorption coefficients[2,10,27] and, in turn, contribute to a larger error in the accuracy of the bandwidth (∼±5 cm^{-1}) and peak maximum (∼±2 cm^{-1}) obtained.

In polystyrene, a given a → b spectrum was recorded with 4 coadditions at each FTIR mirror position using the 16 cm^{-1} "resolution" setting. Three such spectra were added together to yield the final spectrum used for analysis. In poly(methyl methacrylate), PMMA, individual spectra were recorded with 16 coadditions at each mirror position, again at the 16 cm^{-1} resolution setting. Four such spectra were added together to yield the final spectrum used for analysis.

Time-resolved a → X emission spectra at ∼7850 cm^{-1} were recorded with the same step-scan FT spectrometer described above using a general approach that has likewise been discussed elsewhere.[11] In brief, the spectrometer irradiation source was turned off and, after pulsed laser irradiation of the sensitizer,

TABLE 1: Solvent Effect on the $O_2(a^1\Delta_g) \rightarrow O_2(b^1\Sigma_g^+)$ Absorption Maximum and Bandwidth

solvent	n_D[a]	ϵ[b]	absorption maximum (cm^{-1})[c]	$\Delta\nu$[d] (cm^{-1})	absorption bandwidth (cm^{-1})[e]
methanol	1.329	32.6	5217[e]	−24	86[f]
acetonitrile	1.344	37.5	5224[e]	−17	82[f]
Freon-113	1.358	2.4	5209	−32	63
n-hexane	1.375	1.9	5199	−42	69
tetrahydrofuran	1.407	7.6	5207	−34	84
tetrahydropyran	1.420		5202	−39	83
methylcyclohexane	1.422	2.0	5193	−48	71
1,4-dioxane	1.422	2.2	5212	−29	92
cyclohexane	1.426	2.0	5193	−48	73
1,4-dimethylcyclohexane	1.430		5194	−47	68
CCl_4	1.460	2.2	5195	−46	72
p-xylene	1.495	2.3	5190	−51	73
toluene	1.496	2.4	5191	−50	74
poly(methyl methacrylate)	∼1.50	∼3	5207	−34	65
benzene	1.501	2.3	5197	−44	76
pyridine	1.510	12.4	5194	−47	85
benzonitrile	1.528	25.2	5194	−47	81
polystyrene	∼ 1.60	2.5	5184	−57	77
CS_2	1.627	2.6	5168	−73	90

[a] Solvent refractive index at 20 °C. [b] Solvent static dielectric constant at 20 °C. [c] Error of ±1 cm^{-1}. [d] Spectral shift obtained by subtracting the gas-phase transition energy of 5241 cm^{-1} from the solution phase peak maximum. [e] Error of ±2 cm^{-1}. [f] Error of ±5 cm^{-1}.

the a → X emission was coupled into the interferometer along the same optical axis ordinarily used by the spectrometer irradiation source. The emitted light was then coupled back out of the spectrometer and monitored with a 77 K Ge detector (Edinburgh Instruments model EI-P). Signals thus obtained were then used to construct the interferograms from which the a → X spectra were obtained. The emission profiles obtained were corrected for solvent absorption as well as the spectral response of the instrument/detector. The latter was quantified using a blackbody source. These corrections did not influence the band maxima obtained but resulted in a decrease of ∼1−2 cm^{-1} in the measured bandwidth due principally to the instrument response function.

To quantify the a → b absorption and a → X emission bandwidths, a baseline was first established using portions of the spectrum greater than ∼150 cm^{-1} away from the peak maximum. Thereafter, the full width at half-maximum (fwhm) was obtained by taking the difference in absorbance between the peak maximum and the baseline, dividing this difference by two, and measuring the width of the spectral profile in wavenumbers at that point.

All a → b spectra recorded in liquid solvents were obtained using 1 cm path length cuvettes, with the exception of the data recorded in methanol and acetonitrile. Because of appreciable absorption by the solvent itself at ∼5200 cm^{-1}, the a → b data in methanol and acetonitrile were obtained using a 0.2 cm path length cuvette. For most solvents, the singlet oxygen sensitizer used was 9-fluorenone. The latter was stable over the ∼20−40 min period required to record a spectrum. In methanol and acetonitrile, however, where a higher sensitizer concentration was used to compensate for a shorter sample path length, perinaphthenone was used as the sensitizer and it was necessary to use a flow cell that slowly exchanged the solution over the period required to record a spectrum. In all cases, the sample absorbance was ∼0.8 at the wavelength used to irradiate the sensitizer. For the work with liquid solvents, all experiments were performed at ambient atmospheric pressure and the data were independent of whether air- or oxygen-saturated solutions were used. Solvents were obtained from Aldrich (spectrophotometric or HPLC grade) and used as received.

The polystyrene and poly(methyl methacrylate), PMMA, samples containing 9-fluorenone were prepared as previously described using free-radical bulk polymerization techniques.[28] The amorphous glasses thus obtained were cut and polished to yield samples 4 mm thick. The polystyrene data were recorded from samples that had been equilibrated with air at 1 bar (i.e., ambient atmosphere). In PMMA, however, where the oxygen diffusion coefficient is approximately 1 order of magnitude smaller than that in polystyrene,[29] singlet oxygen signals are easier to detect if higher oxygen concentrations are used to (a) trap a larger percentage of the sensitizer triplet states and (b) produce singlet oxygen over a shorter period of time.[28] To this end, the PMMA samples were equilibrated with oxygen at a pressure of 10 bar prior to recording a given spectrum.

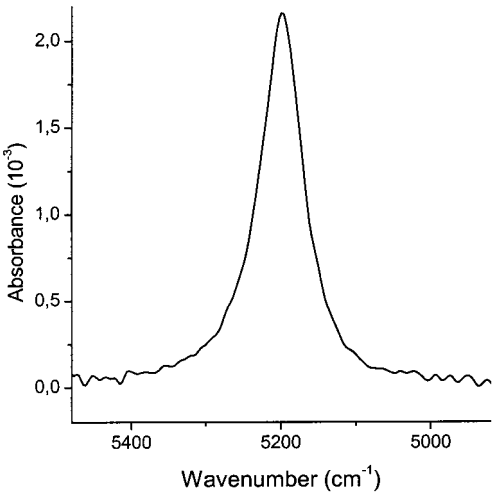

Figure 1. Time-resolved a → b absorption spectrum recorded over a 1 cm path length in air-saturated *n*-hexane.

Results and Discussion

1. Solvent-Dependent a → b Spectral Shifts. For data recorded in a variety of solvents, the $O_2(a^1\Delta_g) \rightarrow O_2(b^1\Sigma_g^+)$ absorption spectrum was always a single distinct band with a peak maximum that could be clearly discerned (Figure 1). Wavenumbers of the peak maxima, obtained from the zero crossings of the first derivatives of the spectra, are listed in Table 1. For the solvents examined, the data reveal solvent-dependent changes in the peak maximum that cover a range of ∼55 cm^{-1}.

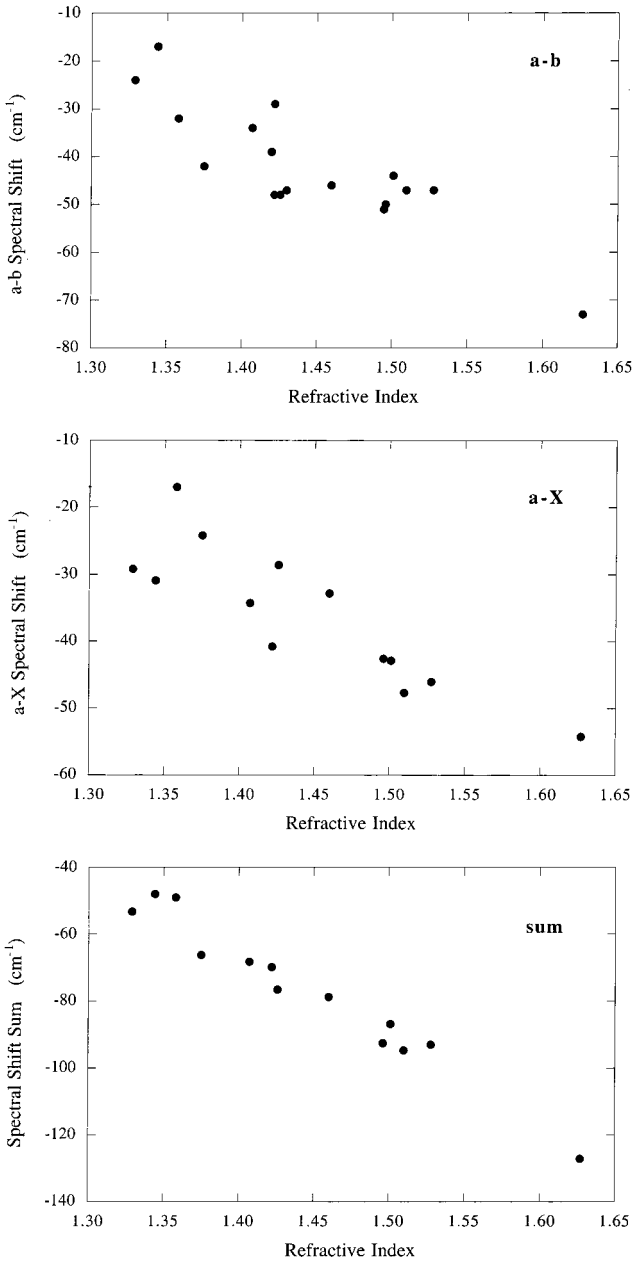

Figure 2. (a, top) Plot of the a → b spectral shift against the refractive index of the solvent in which oxygen is dissolved. (b, middle) Plot of the a → X spectral shift against the refractive index of the solvent in which oxygen is dissolved. (c, bottom) Sum of the a → b and a → X spectral shifts against the refractive index of the solvent in which oxygen is dissolved.

Assuming that the b → a emission maximum recorded in the gas phase provides a reasonable estimate of the gas-phase a → b absorption maximum (i.e., the gas-phase a−b Stokes shift will be very small, arguably much less than the already small Stokes shift in solution[11]), one can obtain a solvent-dependent spectral shift, $\Delta\nu$, by taking the difference between the solution and gas-phase peak maxima. Using the gas-phase b → a emission maximum reported by Noxon of 5241 cm^{-1},[30] values of $\Delta\nu$ obtained for the solvents studied cover the range −17 to −73 cm^{-1} (Table 1).

In previous studies of solvent effects on both a → X and b → a spectral shifts,[6−8] it has been noted that the data correlate reasonably well with the solvent refractive index or with functions of the solvent refractive index that are related to the solvent electronic polarizability. Specifically, the extent of the spectral shift generally increases with an increase in the solvent refractive index or, alternatively, with an increase in the solvent polarizability. As explained in some of our earlier reports, however, caution must be exercised in ascribing physical meaning to these correlations or, perhaps more appropriately, trends.[19,20] Nevertheless, with this caveat in mind, we have likewise plotted the present a → b data against the solvent refractive index and find a similar trend (Figure 2a).[31]

TABLE 2: Solvent Effect on the $O_2(a^1\Delta_g) \rightarrow O_2(X^3\Sigma_g^-)$ Emission Maximum and Bandwidth

solvent	emission maximum (cm^{-1})	$\Delta\nu^a$ (cm^{-1})	emission bandwidth (cm^{-1})
methanol	7853.2[b]	−29.2	125.4[b]
acetonitrile	7851.5[b]	−30.9	125.3[b]
Freon-113	7865.4[c]	−17.0	92.5[c]
n-hexane	7858.2[b]	−24.2	97.6[b]
tetrahydrofuran	7848.1[b]	−34.3	118.5[b]
1,4-dioxane	7841.6[b]	−40.8	119.3[b]
cyclohexane	7853.8[b]	−28.6	101.8[b]
CCl_4	7849.2[c] 7850.1[b]	−32.8	102.8[c] 102.8[b]
toluene	7839.9[b] 7839.7[d]	−42.6	113.3[b] 112.5[d]
poly(methyl methacrylate)	7848.2[d]	−34.2	99.0[d]
benzene	7839.5[b]	−42.9	115.9[b]
pyridine	7834.7[d]	−47.7	116.8[d]
benzonitrile	7836.3[b]	−46.1	106.3[b]
polystyrene	7837.3[d]	−45.1	110.0[d]
CS_2	7827.3[c] 7829.2[b]	−54.2	121.6[c] 122.2[b]

[a] Spectral shift obtained by subtracting the gas-phase transition energy of 7882.4 cm^{-1} from the mean solution phase peak maximum. [b] From Wessels and Rodgers.[7] [c] From Macpherson et al.[6] [d] Determined in the present study (±0.5 cm^{-1} on band maximum and ±2.0 cm^{-1} on bandwidth).

Most of the solvents used in our present a → b study have also been used in independent studies of the a → X emission. In Table 2 we list a → X data from these solvents that have likewise been obtained in Fourier transform spectroscopic studies. In Figure 2b, these a → X spectral shifts are plotted against the solvent refractive index. The trend observed in this case is very similar to that observed with the a → b data shown in Figure 2a. It is important to note at this juncture that the data shown in Figure 2b include many of the so-called "anomalous" points identified in the study of Wessels and Rodgers[7] that "spoiled" what, for an extensive list of solvents, was a reasonable correlation of $\Delta\nu$ with the refractive index.

As illustrated in Scheme 1, both the a → X and a → b transitions originate from an oxygen molecule in the $a^1\Delta_g$ state that is in *equilibrium* with the surrounding solvent and, hence, is stabilized as a consequence of both the inertial and optical polarization vectors. In the final, Franck−Condon state that defines the energy, and hence the peak maximum, of a given transition, the oxygen molecule is *not in equilibrium* with the surrounding solvent. In this case, stabilization derives principally from optical polarization vectors because the inertial vectors have not yet had the chance to respond to the new solute charge distribution. In an earlier study, we demonstrated for three solvents (CS_2, CCl_4, and Freon-113) that, for a given solvent, the difference between the equilibrium and nonequilibrium solvation energies of the $O_2(a^1\Delta_g)$ and $O_2(b^1\Sigma_g^+)$ states is small ($\leq$3 cm^{-1}).[11] Unfortunately, because of the extremely short $O_2(b^1\Sigma_g^+)$ lifetime in solvents containing C−H and O−H bonds, it is difficult to monitor $O_2(b^1\Sigma_g^+)$ and hence quantify this same difference between equilibrium and nonequilibrium solvation energies in a wider range of solvents, particularly solvents in which specific solvent effects may be more pronounced. Irrespective of whether such a small difference in solvation

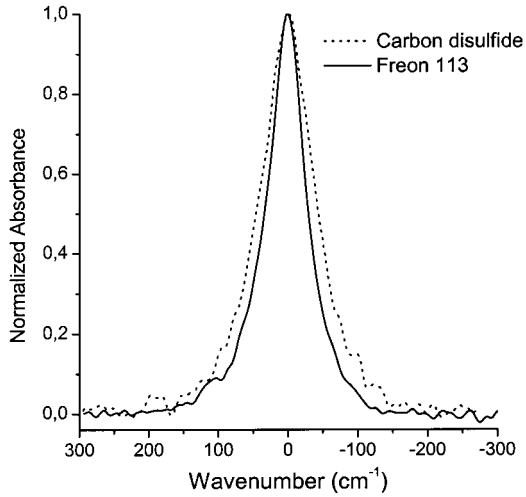

Figure 3. a → b absorption spectrum recorded in CS_2 superimposed on the a → b absorption spectrum recorded in Freon-113 ($CF_2ClCFCl_2$). In each case, the band maximum defines the "zero point" on the *x*-axis.

energies is also found in other solvents, it is nevertheless reasonable to expect that, upon going from one solvent to another, the transition energy from a solvent-equilibrated to a nonequilibrated state may not correlate well with functions that depend only on the solvent refractive index (e.g., Figure 2a,b). Rather, one should ideally try to find the appropriate expression(s) that accounts for the effects of both the optical and inertial vectors, $\mathbf{P}_{op}$ and $\mathbf{P}_{in}$, among other things. This has been accomplished reasonably well in our preliminary study of the a → X transition.[20] On the other hand, if one could examine the hypothetical transition from a nonequilibrated state of oxygen to another nonequilibrated state, one should see a much better correlation of the transition energy with functions that depend only on the solvent refractive index. Such a hypothetical transition can be modeled simply by taking the sum of the a → b and a → X spectral shifts, and a plot of this sum against the solvent refractive index indeed shows a remarkably good correlation (Figure 2c). In conclusion, the data shown in Figure 2 clearly demonstrate the importance of considering the effects of equilibrium and nonequilibrium solvation when interpreting the effect of solvent on transitions between the $X^3\Sigma_g^-$, $a^1\Delta_g$, and $b^1\Sigma_g^+$ states of oxygen.

2. Solvent-Dependent a → b Absorption Bandwidths. The a → b absorption spectra recorded also indicate a clear solvent effect on the spectral bandwidth. This is illustrated in Figure 3 where one spectrum has been superimposed upon another using the peak maximum as a center point. For the solvents examined in this study, solvent-dependent changes in the full width at half-maximum (fwhm) of the band cover a range of ~30 cm^{-1} (Table 1).

Keeping in mind the limitations mentioned in the previous section and discussed in our earlier work,[19,20] it is useful to examine how these a → b spectral bandwidths correlate with a number of parameters.

(a) Bandwidth against Solvent Refractive Index. Plots such as those shown in Figure 2, in which a → b and a → X spectral shifts are examined as a function of the solvent refractive index, prompt us to similarly examine how bandwidths depend on the solvent refractive index. In this case (Figure 4), it is clear that the data neither correlate with the refractive index nor can one even claim to discern an overall trend.[31] On the other hand, it is interesting to note that the same solvents identified by Wessels and Rodgers[7] as being "anomalous" in that they "spoiled" the correlation between the a → X spectral shift and the refractive

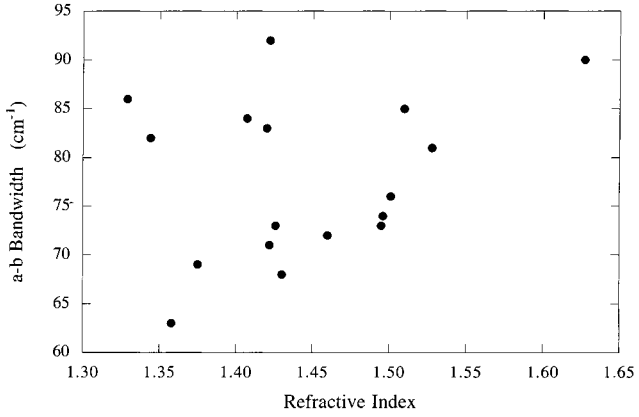

Figure 4. Plot of the a → b spectral bandwidth (fwhm) against the refractive index of the solvent in which oxygen is dissolved.[31] The five points in the upper left quadrant of this plot correspond to data obtained in acetonitrile, methanol, dioxane, tetrahydrofuran, and tetrahydropyran. The first four of these solvents were identified by Wessels and Rodgers[7] as being "anomalous" in their study of the a → X spectral shift (see text). Wessels and Rodgers did not record a → X data in tetrahydropyran.

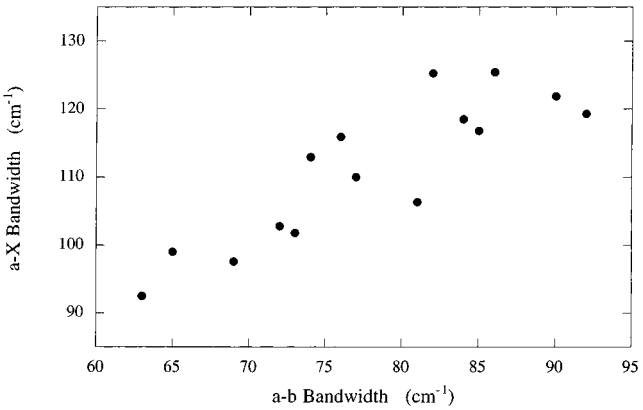

Figure 5. Plot of the a → X spectral bandwidth (fwhm) against the a → b spectral bandwidth (fwhm) for data recorded from 13 different liquid solvents and 2 polymer glasses (PMMA and polystyrene).

index, could arguably be claimed to likewise "spoil" the present plot (see Figure 4 caption). It is more important to note that, for the cases where common solvents have been examined, a plot of the a → X bandwidth (Table 2) against solvent refractive index resembles the corresponding plot of the a → b bandwidth against refractive index. This is illustrated in Figure 5 where the a → X bandwidth is shown to correlate reasonably well with the a → b bandwidth. Thus, it appears that whatever the solvent does to influence these bandwidths, the effect on the a → X transition is very similar to that on the a → b transition.

(b) Bandwidth against Spectral Shift. In this case, we consider the notion, expressed in an earlier study,[7] that the "strength" of the solvent−solute interaction as manifested in the spectral shift is similarly manifested in the spectral bandwidth. In plots of the a → X spectral shift against the a → X bandwidth, both Macpherson et al.[6] as well as Wessels and Rodgers[7] noted a crude, but discernible, trend; it was observed that the a → X bandwidth is generally larger in those solvents that give rise to the largest spectral shift. In our present study on the a → b transition, the analogous plot shows data that are quite scattered and indicate the lack of any correlation between the a → b bandwidth and a → b spectral shift (Figure 6). Once again, however, it is interesting to note that upon discounting data from the so-called "anomalous" solvents of Wessels and Rodgers,[7] one would indeed be able to claim that the a → b bandwidth is

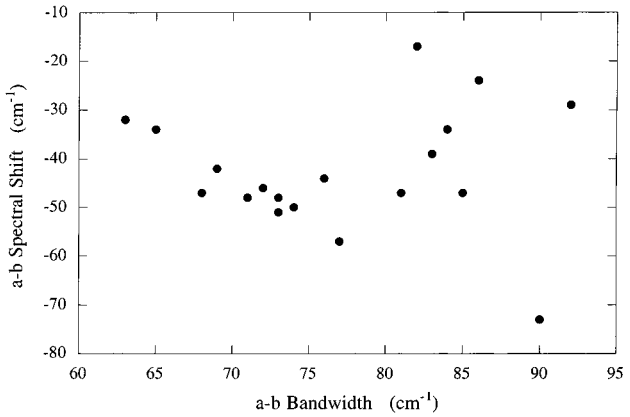

Figure 6. Plot of the a → b spectral shift against the a → b spectral bandwidth (fwhm). The five points in the upper right quadrant of this plot correspond to data obtained in acetonitrile, methanol, dioxane, tetrahydrofuran, and tetrahydropyran.

generally larger in solvents that give rise to the largest a → b spectral shift (see Figure 6 caption). Pertinent aspects of this issue are further developed in Section 4 below.

(c) Bandwidth as a Function of Molecular Symmetry. Some of the molecules shown in Table 1 were chosen to test the following hypothesis: one phenomenon that will influence the a → b spectral bandwidth is the homogeneity of the first solvation shell and this, in turn, could depend on the symmetry of the individual solvent molecules. In this regard, we thought it would be useful to examine three sets of solvents based on a substituted six-member ring structure: (1) cyclohexane, methylcyclohexane, and 1,4-dimethylcyclohexane, (2) benzene, toluene, and *p*-xylene, and (3) cyclohexane, tetrahydropyran, and 1,4-dioxane. With this line of reasoning, the expectation was that, upon disrupting the symmetry of a given solvent molecule (i.e., the second molecule in a given set), one should see an increase in the a → b bandwidth. Upon restoring some of the symmetry back into the system (i.e., the third molecule in a given set), the a → b bandwidth should, in turn, decrease. The data in Table 1 indicate, however, that this expectation was not fulfilled. Thus, in this case, we conclude that either the molecules chosen to test the hypothesis were inappropriate or, for the molecules chosen, the effect of molecular symmetry on the homogeneity of the first solvation shell is small compared to other parameters which influence the bandwidth.

3. Symmetry of the a → b Absorption Band. One method by which one could arguably assess the homogeneity of the environment to which oxygen is exposed in a given solvent is to examine not just the bandwidth, but the symmetry of the band about the peak maximum. As illustrated in Figure 7, the a → b band is reasonably symmetric in some solvents, whereas in other solvents, the asymmetry can be quite pronounced. To assess the symmetry of these absorption bands, or lack thereof, a Lorentzian fitting function was applied to the data (dashed line in Figure 7). The Lorentzian profile is symmetrical about the peak maximum and, in general, is expected to adequately model an inhomogeneously broadened band.[32] It is again interesting to note that dioxane and some of the other so-called "anomalous" solvents of Wessels and Rodgers[7] tend to have comparatively asymmetrical band profiles.

Unfortunately, attempts to use the symmetry of the a → b band to assess the homogeneity of the perturbing solvent environment are likely to be complicated by another solvent-dependent variable that will likewise influence the band shape. In a number of gas-phase a → X studies, spectra have been recorded in which P, Q, and R rotational branches are resolved,

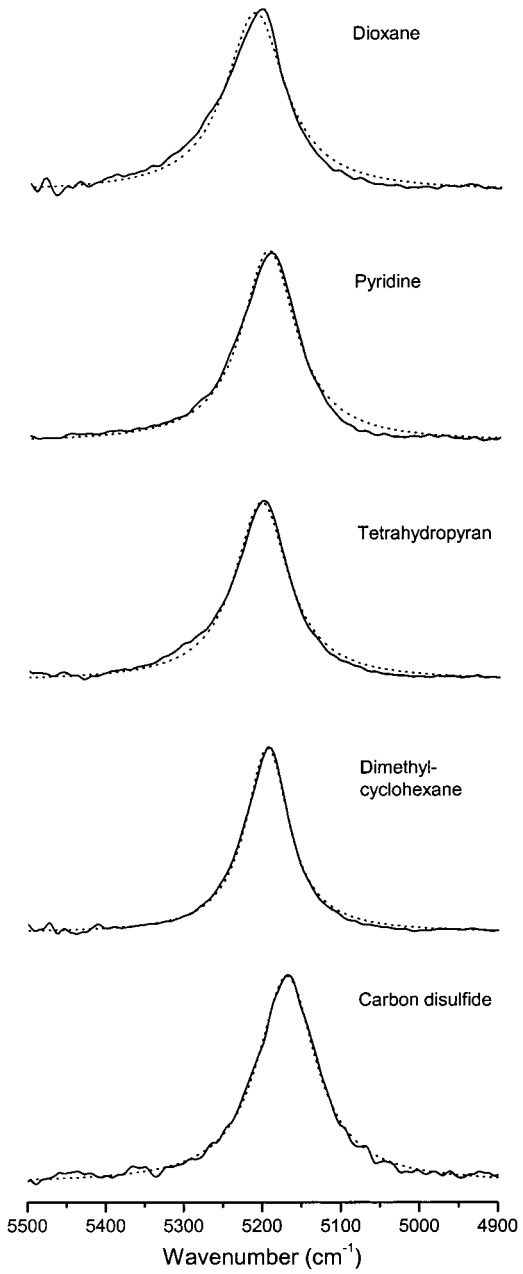

Figure 7. a → b absorption spectra recorded in five solvents illustrating bands that are reasonably symmetric about the band maximum as well as bands that are asymmetric about the band maximum. A standard by which symmetry can be assessed is provided by the Lorentzian profile (dashed line).

or partially resolved.[33,34] Moreover, the relative intensities of the P and R branches are not equivalent. In a → X emission studies performed at moderately high gas pressures, it has also been shown that these rotational branches are superimposed onto a continuum that, in turn, contributes to the overall profile of the spectrum recorded.[34] On the basis of these observations, Macpherson et al.[6] have assumed that, in their study of the symmetry of solution-phase a → X spectra, the data reflect contributions from the P and R branches that can be quite different. In a study of the b → a emission at moderate gas pressures, Fink et al.[35] have likewise observed this superposition of asymmetrical P and R branches onto a continuum. Thus, by extension, our a → b band shapes may reflect not just a general solvent-dependent inhomogeneous broadening, but may also reflect solvent-dependent changes in the relative intensities of underlying P and R rotational bands.

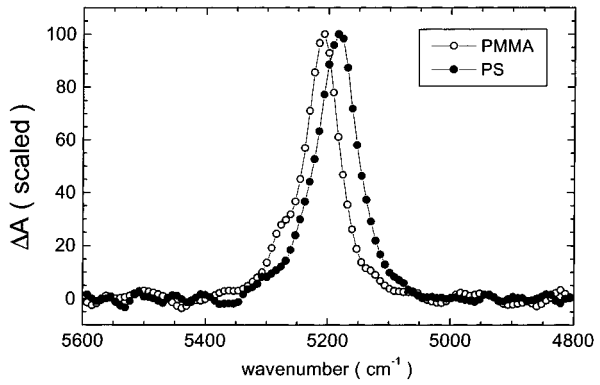

Figure 8. a → b absorption spectra recorded in poly(methyl methacrylate), PMMA, and polystyrene, PS, glasses. The symbols on each spectrum are simply markers placed at intervals of ~7 cm^{-1}, and are not associated with the spectral resolution available. Reprinted with permission from Ogilby et al.[42]

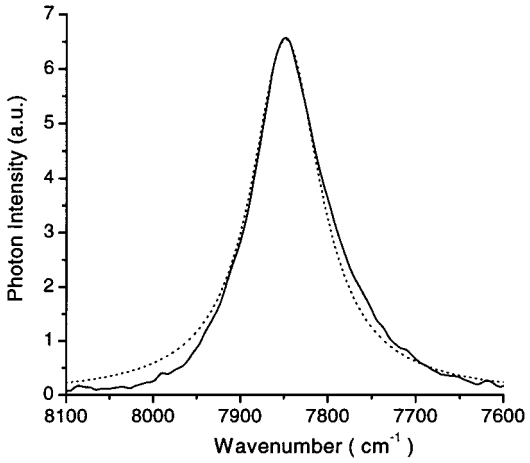

Figure 9. a → X emission spectrum recorded in a poly(methyl methacrylate) glass (solid line). A standard by which the band symmetry can be assessed is provided by the Lorentzian profile (dashed line).

Of all the a → b spectra we have recorded, the spectrum recorded from a poly(methyl methacrylate) glass stands out as being the most asymmetrical (Figure 8). In contrast, a → b data recorded from a polystyrene glass appear no different than those from liquid solutions. Given that the diffusion coefficient of oxygen in PMMA is approximately 1 order of magnitude smaller than that in polystyrene[29] and approximately 3 orders of magnitude smaller than those in typical liquid solvents,[36,37] one might argue that the PMMA spectrum reflects the sorption of oxygen in different sites in the polymer matrix (e.g., the PMMA spectrum can be modeled as the sum of two separate Lorentzians). If true, then this feature of the a → b spectrum recorded in PMMA should likewise be manifested in the a → X spectrum recorded under the same conditions. Although distinctly asymmetrical, the a → X spectrum recorded from PMMA (Figure 9) nevertheless more resembles those recorded from other solvents and certainly lacks the distinctive "shoulder" seen in the PMMA a → b absorption spectrum. Thus, the latter most likely reflects a phenomenon other than the sorption of oxygen in different sites. For example, one possibility is that the steady-state "background" spectrum of the PMMA matrix used to normalize the time-resolved a → b spectrum may not accurately represent the actual spectrum of PMMA under conditions in which heat from a pulsed laser is being deposited into the matrix. Indeed, PMMA is a unique solvent for this study in that it has a relatively strong absorption band at ~5250 cm^{-1} that lies right on the edge of the a → b absorption profile. Thus, a slight temperature-dependent change in the position of this PMMA band would result in an inaccurate background normalization which, in turn, could yield the shoulder observed in the a → b spectrum. We have indeed documented similar laser-induced, temperature-dependent changes in the IR absorption bands of other solvent systems.[38] Nevertheless, more experiments need to be performed on this issue to justify further discussion.

Although the a → b spectrum recorded in PMMA shows a definite shoulder, the latter does not appear to appreciably influence the bandwidth we ascertain for the principal peak. Thus, for the data shown in Figures 5 and 6, we have chosen not to exclude the PMMA result, despite our own cautions about comparing data recorded at high oxygen pressures to those recorded at low oxygen pressures.[11] It is important to note, however, that any conclusions we draw regarding possible trends in Figures 5 and 6, or the lack thereof, are independent of whether the polymer data are included.

4. Solvation Model. The comments made in this section supplement those made in our earlier studies on the role of the solvent in influencing spectral transitions in oxygen,[11,20] but in particular, we focus here on the issue of equilibrium and nonequilibrium solvation. The data obtained in the present study are consistent with the following statements.

a → b and a → X spectral shifts reflect the effects of both nonequilibrium as well as equilibrium solvation. As discussed in Section 1, both the a → X and a → b transitions originate from a state that is in equilibrium with the surrounding solvent and thus is stabilized as a consequence of both the inertial and optical polarization vectors. However, in the final, Franck−Condon state for each transition, oxygen is not in equilibrium with the surrounding solvent. Stabilization of these latter states derives principally from the optical polarization vectors. It is thus not surprising that the transition energies, or solvent-dependent spectral shifts $\Delta\nu$, do not correlate well with parameters that only reflect optical polarization vectors (i.e., solvent refractive index). This point is not only illustrated in Figure 2a,b, but was manifested in the work of Wessels and Rodgers[7] through the so-called "anomalous" solvents. This interpretation can be tested by "removing" the effect of solvent on the equilibrated $a^1\Delta_g$ state and examining the hypothetical transition from the nonequilibrated $X^3\Sigma_g^-$ state to the nonequilibrated $b^1\Sigma_g^+$ state obtained as a sum of the a → X and a → b spectral shifts. For this latter hypothetical transition, one should specifically see a much better correlation with the solvent refractive index, and this is indeed the case as illustrated in Figure 2c. Thus, any model that accounts for the effect of solvent on transition energies in dissolved oxygen must consider the effects of equilibrium solvation on the initial state in the transition.

a → b and a → X spectral bandwidths are principally a phenomenon of equilibrium solvation. As a starting point for this discussion, we note that, in solution, both the a → b and a → X transitions will be inhomogeneously broadened.[32,39,40] Thus, we can say that these transitions originate from $O_2(a^1\Delta_g)$ molecules distributed over a range of solvation sites, each differing slightly from the next by the relative orientations of oxygen and the surrounding solvent molecules. In this description, the inertial polarization vectors clearly play a key role. Thus, it is not surprising that, unlike the data on a → b spectral shifts (Figure 2a), there is no discernible trend when the a → b bandwidth is plotted against the solvent refractive index (Figure 4). Moreover, it is gratifying to see that there is a reasonable correlation between the a → X and a → b bandwidths (Figure 5). This indicates that, whatever the solvent does to influence

these bandwidths, the effect on the a → X transition is very similar to that on the a → b transition. Of course, the latter is to be expected if, in defining the bandwidths, the principal effect of the solvent is to influence the one state common to both the a → X and a → b transitions; the solvent-equilibrated $a^1\Delta_g$ state.

A corollary of these statements on the effects of solvent on the a → b transition is that one should not expect a correlation between the a → b bandwidth and the a → b spectral shift. The data shown in Figure 6 indeed support this expectation.

Conclusions

The $a^1\Delta_g \rightarrow b^1\Sigma_g^+$ absorption spectrum of molecular oxygen was recorded in 19 solvents, and solvent-dependent changes in the full-width-at-half-maximum of this absorption band as well as the position of the band maximum were quantified. When considered along with earlier results on the $O_2(a^1\Delta_g) \rightarrow O_2(X^3\Sigma_g^-)$ transition, the present data clearly demonstrate the importance of considering equilibrium and nonequilibrium solvation in models of the interaction between oxygen and the surrounding solvent. The data presented indicate that the bandwidths of the $O_2(a^1\Delta_g) \rightarrow O_2(b^1\Sigma_g^+)$ and $O_2(a^1\Delta_g) \rightarrow O_2(X^3\Sigma_g^-)$ transitions are principally a phenomenon of equilibrium solvation, whereas the associated solvent-dependent spectral shifts depend on both equilibrium and nonequilibrium solvation. Along with our earlier cautions about ascribing physical meaning to the trends observed in plots of a → X spectral shifts against the solvent refractive index,[19,20] this present perspective thus clarifies the issue of the so-called "anomalous" solvents identified in the a → X study of Wessels and Rodgers.[7]

In a series of recent studies, we have established the framework of an ab initio computational approach that can be used to model the effect of solvent on electronic transitions in oxygen.[11,20−23] As demanded by the results of the present a → b study, this computational approach allows one to distinguish the effects of equilibrium and nonequilibrium solvation. It is now necessary to establish whether this ab initio tool, in its present form, can satisfactorily model not just the spectral shift and bandwidth data reported herein, but the effect of solvent on the rate constants of radiative transitions between oxygen's low-lying electronic states.[3,41] The latter, of course, are also an integral component of defining the profile of a given spectral band; within an inhomogeneously broadened band, a transition of a given energy must be weighted by the appropriate transition probability. It will be particularly important in this regard to see how well the asymmetry in a given absorption band can be modeled. A critical component with respect to this point will be the extent to which one can use a molecular dynamics simulation, for example, to establish the coordinates of pertinent oxygen−solvent orientations in a solvation shell that can be locally inhomogeneous.

Acknowledgment. This work was supported by grants from the Danish Natural Science Research Council. The authors thank Tina D. Poulsen and Alisdair N. Macpherson for comments on this manuscript.

References and Notes

(1) Ogilby, P. R. *Acc. Chem. Res.* **1999**, *32*, 512−519.

(2) Keszthelyi, T.; Weldon, D.; Andersen, T. N.; Poulsen, T. D.; Mikkelsen, K. V.; Ogilby, P. R. *Photochem. Photobiol.* **1999**, *70*, 531−539.

(3) Hild, M.; Schmidt, R. *J. Phys. Chem. A.* **1999**, *103*, 6091−6096.

(4) Bromberg, A.; Foote, C. S. *J. Phys. Chem.* **1989**, *93*, 3968−3969.

(5) Byteva, I. M.; Gurinovich, G. P.; Losev, A. P.; Mudryi, A. V. *Opt. Spektros.* **1990**, *68*, 317−319.

(6) Macpherson, A. N.; Truscott, T. G.; Turner, P. H. *J. Chem. Soc., Faraday Trans.* **1994**, *90*, 1065−1072.

(7) Wessels, J. M.; Rodgers, M. A. J. *J. Phys. Chem.* **1995**, *99*, 17586−17592.

(8) Weldon, D.; Wang, B.; Poulsen, T. D.; Mikkelsen, K. V.; Ogilby, P. R. *J. Phys. Chem. A* **1998**, *102*, 1498−1500.

(9) Schmidt, R.; Bodesheim, M. *J. Phys. Chem. A* **1998**, *102*, 4769−4774.

(10) Weldon, D.; Ogilby, P. R. *J. Am. Chem. Soc.* **1998**, *120*, 12978−12979.

(11) Keszthelyi, T.; Poulsen, T. D.; Ogilby, P. R.; Mikkelsen, K. V. *J. Phys. Chem. A* **2000**, *104*, 10550−10555.

(12) Bayliss, N. S.; McRae, E. G. *J. Phys. Chem.* **1954**, *58*, 1002−1006.

(13) Marcus, R. A. *J. Chem. Phys.* **1956**, *24*, 979−989.

(14) Kim, H. J.; Hynes, J. T. *J. Chem. Phys.* **1990**, *93*, 5194−5210.

(15) Reichardt, C. *Solvents and Solvent Effects in Organic Chemistry*, 2nd ed.; VCH: Weinheim, 1988.

(16) Lakowicz, J. R. *Principles of Fluorescence Spectroscopy*; Kluwer Academic/Plenum: New York, 1999.

(17) Schmidt, R. *J. Phys. Chem.* **1996**, *100*, 8049−8052.

(18) Lin, S. H.; Lewis, J.; Moore, T. A. *J. Photochem. Photobiol. A* **1991**, *56*, 25−34.

(19) Poulsen, T. D.; Ogilby, P. R.; Mikkelsen, K. V. *J. Phys. Chem. A* **1998**, *102*, 8970−8973.

(20) Poulsen, T. D.; Ogilby, P. R.; Mikkelsen, K. V. *J. Phys. Chem. A* **1999**, *103*, 3418−3422.

(21) Poulsen, T. D.; Kongsted, J.; Osted, A.; Ogilby, P. R.; Mikkelsen, K. V. *J. Chem. Phys.* **2001**, *115*, 2393−2400.

(22) Poulsen, T. D.; Ogilby, P. R.; Mikkelsen, K. V. *J. Chem. Phys.* **2001**, *115*, 7843−7851.

(23) Poulsen, T. D.; Ogilby, P. R.; Mikkelsen, K. V. *J. Chem. Phys.* **2002**, *116*, 3730−3738.

(24) Andersen, L. K.; Ogilby, P. R. *Photochem. Photobiol.* **2001**, *73*, 489−492.

(25) Guelachvili, G.; Rao, K. N. *Handbook of Infrared Standards II*; Academic Press: Boston, 1993.

(26) Wilkinson, F.; Helman, W. P.; Ross, A. B. *J. Phys. Chem. Ref. Data* **1995**, *24*, 663−1021.

(27) Weldon, D.; Poulsen, T. D.; Mikkelsen, K. V.; Ogilby, P. R. *Photochem. Photobiol.* **1999**, *70*, 369−379.

(28) Clough, R. L.; Dillon, M. P.; Iu, K.-K.; Ogilby, P. R. *Macromolecules* **1989**, *22*, 3620−3628.

(29) Poulsen, L.; Ogilby, P. R. *J. Phys. Chem., A* **2000**, *104*, 2573−2580.

(30) Noxon, J. F. *Can. J. Phys.* **1961**, *39*, 1110−1119.

(31) The refractive index of PMMA and polystyrene glasses can vary from one sample to the next, and the values listed in Table 1 are only approximations. Thus, the polymer data are excluded from plots in which the refractive index is a variable.

(32) Steinfeld, J. I. *Molecules and Radiation: An Introduction to Modern Molecular Spectroscopy*; The MIT Press: Cambridge, 1974.

(33) Whitlow, S. H.; Findlay, F. D. *Can. J. Chem.* **1967**, *45*, 2087−2091.

(34) Wildt, J.; Fink, E. H.; Biggs, P.; Wayne, R. P.; Vilesov, A. F. *Chem. Phys.* **1992**, *159*, 127−140.

(35) Fink, E. H.; Setzer, K. D.; Wildt, J.; Ramsay, D. A.; Vervloet, M. *Int. J. Quantum Chem.* **1991**, *39*, 287−298.

(36) Kowert, B. A.; Dang, N. C. *J. Phys. Chem. A* **1999**, *103*, 779−781.

(37) Tsushima, M.; Tokuda, K.; Ohsaka, T. *Anal. Chem.* **1994**, *66*, 4551−4556.

(38) Andersen, L. K.; Ogilby, P. R. *J. Phys. Chem.* Submitted for publication.

(39) Myers, A. B. *Annu. Rev. Phys. Chem.* **1998**, *49*, 267−295.

(40) Leontidis, E.; Suter, U. W.; Schütz, M.; Lüthi, H.-P.; Renn, A.; Wild, U. P. *J. Am. Chem. Soc.* **1995**, *117*, 7493−7507.

(41) Scurlock, R. D.; Nonell, S.; Braslavsky, S. E.; Ogilby, P. R. *J. Phys. Chem.* **1995**, *99*, 3521−3526.

(42) Ogilby, P. R.; Andersen, L. K.; Dam, N.; Frederiksen, P. K.; Jørgensen, M.; Poulsen, L. *Polym. Prepr.* **2001**, *42* (1), 407−408.